



## FORMULATION AND CHARACTERIZATION OF MICROEMULSION OF POORLY WATER SOLUBLE DRUG GLYBURIDE

Prabhakar Vishvakarma\*, K. Saravanan, Saurabh Sharma

Department of Pharmacy, Bhagwant University, Ajmer, Rajasthan, India

\*Corresponding author: [prabhakar.vishvakarma7788@gmail.com](mailto:prabhakar.vishvakarma7788@gmail.com)

### ABSTRACT

The objective of the present investigation was to develop and evaluate microemulsifying drug delivery system for improving the delivery of a BCS class II antidiabetic agent, glyburide (GLY). The solubility of glyburide in oils, surfactants and co-surfactants (Capmul MCM: Tween80: Span20) was evaluated to identify the components of the microemulsion. Pseudoternary phase diagrams diagram was utilized to identify the optimal excipient composition to formulate the microemulsion system and the area of microemulsion existence. Glyburide microemulsion was characterized by refractive index, optical clarity, assay, dye solubility, viscosity, surface tension, pH, drug content, polydispersity index, drug loading, entrapment efficiency, particle size, zeta Potential, scanning electron microscopy (SEM), differential scanning calorimetry measurements (DSC) and viscosity. The *in vitro* dissolution profile of glyburide microemulsion was evaluated the pure drug in pH 7.4 buffers. The chemical stability of glyburide in microemulsion was determined as per the International Council for Harmonisation (ICH) guidelines.

**Keywords:** Glyburide, Microemulsion, Solubility, Stability, SEM, DSC, FTIR.

### 1. INTRODUCTION

Glyburide (GLY) or glibenclamide is a second generation sulfonylurea used for treat non insulin-dependent diabetes. It is one of the mostly prescribed long-acting antihyperglycemic agents [1]. Glyburide is classified as a BCS class II drug, which means that it has high permeability and low water solubility [2]. The poor solubility of glyburide in water is the reason for its low dissolution rate, which ultimately leads to variable absorption of glyburide. In addition, there are reports that GLY shows large differences in the individual bioavailability and bioequivalence of the marketed products [3] Thus, it can be concluded that *in vivo* performance of glyburide depend on its dissolution rate and the bioavailability. Given this, researchers have attempted different techniques to improve the dissolution rate. Eventually, the *in vivo* performance of glyburide, solid dispersion, cyclodextrin complexation, and permeation enhancers has been established in improving *in vitro* and *in vivo* performance of glyburide. However, to date, the potential of microemulsions has not been established in the delivery of glyburide [4]. Researches also stated that the microemulsion formulation Glyburide, a poorly water-soluble drug, significantly

increased oral absorption, irrespective of whether the subject was fed [5]. Improved absorption from a microemulsion is probably due to the incorporation of the drug into microemulsion droplets. Smaller microemulsion droplets result in an increased specific surface area and enhanced membrane permeability of the drug *via* solubilization of certain membrane components and pore-formation. All these factors lead to enhanced contact with the gastrointestinal tract. Another important factor is the inner polarity of droplets, which is directed by the hydrophilic-lipophilic balance of surfactant used. A change in droplet polarity may affect the form of the drug and surfactant on the droplet interface and alter drug release [6]. Microemulsions have also been acknowledged as topical [7], transdermal [8] and parenteral drug delivery systems [9] and several studies have reported the use of a microemulsion as an oral drug delivery system [10]. In this work, different pre-microemulsion and microemulsion formulations were prepared to improve glyburide availability. This was done by the selection of the most suitable microemulsion ingredients that reached the highest solubilization of glyburide. Then, the chosen microemulsion formulations were characterized to help in selecting the most suitable formulation.

## 2. MATERIAL AND METHODS

Glyburide was kindly provided as a gift sample by Cipla Pharmaceuticals (Mumbai, India). Labrafac CC (Colorcon Asia, Mumbai, India), Capmul MCM (Indchem International, Mumbai, India), cotton seed oil, sunflower oil and soybean oil; surfactants, *i.e.*, Captex-355, Cremophor EL, PEG 400, Labrafil (all AR grade) were purchased from Merck (Mumbai, India) and Tween-80 (SD fine chemicals Private Limited, Gujarat, India); and co-surfactants, *i.e.*, *n*-butanol, span-20 and propylene glycol (all AR grade) were purchased from Merck (Mumbai, India). Hydrochloric acid and potassium dihydrogen phosphate (all AR grade) were purchased from s.d. Fine Chemicals (Mumbai, India).

### 2.1. Solubility studies of glyburide in different oils, surfactants, and co-surfactants

The solubility of glyburide was examined in different oils, *i.e.*, Labrafac CC, Capmul MCM cotton seed oil, sunflower oil and soybean oil; surfactants, *i.e.*, Captex-355, Cremophor EL, Tween-80, Labrafil and PEG 400; and co-surfactants, *i.e.*, *n*-butanol, span-20 and propylene glycol. The equilibrium solubility method was performed. Briefly, an excess amount of glyburide was added to 10 ml of each solvent (the aforementioned oils, surfactants, and co-surfactants) in 30 ml screw capped

vials and the whole mixture was mixed by vortexing. The vials were then shaken at 37°C for 72 h at 100 rpm in a thermostatically controlled water bath shaker (Weiss Gallenkamp, Loughborough, UK). Then, the supernatant layer was separated and subjected to centrifugation at 3,000 rpm for 5 min in order to remove the un-dissolved drug. Samples of these solutions were then collected and the drug concentration was determined spectrophotometrically at 301 nm against a suitable blank of DMSO using an ultraviolet spectrophotometer SP6-550 (Pye Unicam, Cambridge, England). All experiments were performed in triplicate [11].

### 2.2. Oils, surfactants and co-surfactants loading at different percentages in Glyburide micro-emulsion

Predetermined amounts of the drug were dissolved in the required quantity of oil. Surfactant and co-surfactant were added to the above mixture as a fixed ratio. Distilled water was added gradually with continuous stirring, which resulted in the formulation of a transparent and homogenous microemulsion. Parameters optimized for the preparation of microemulsion were the type and concentration of the oil phase, surfactant and co-surfactant [11].

**Table 1: Factor combination as per the chosen experimental design**

S. NO	Formulation code	Drug (Glyburide)	Aqueous region %	Amphiphilic region %	Surfactant : co-surfactant	Oil %
			Water		Tween80 : Span20	Capmul MCM
1	F1	5mg	50	40	1:9	10
2	F2	5mg	48	40	2:8	12
3	F3	5mg	46	40	3:7	14
4	F4	5mg	44	40	4:6	16
5	F5	5mg	42	40	5:5	18
6	F6	5mg	40	40	6:4	20
7	F7	5mg	38	40	7:3	22
8	F8	5mg	36	40	8:2	24
9	F9	5mg	34	40	9:1	26

### 2.3. Pseudoternary phase diagram study

Pseudoternary phase diagrams of oil, water, and surfactant/co-surfactants (S/Cos) mixtures are constructed at fixed surfactant/co-surfactant weight ratios. Phase diagrams are obtained by mixing of the ingredients, which shall be pre-weighed into glass vials and titrated with water and stirred well at room temperature. Formation of the monophasic/biphasic

system is confirmed by visual inspection. In case turbidity appears followed by a phase separation, the samples shall be considered as biphasic. In case monophasic, clear and transparent mixtures are visualized after stirring; the samples shall be marked as points in the phase diagram. The area covered by these points is considered as the microemulsion region of existence [12].

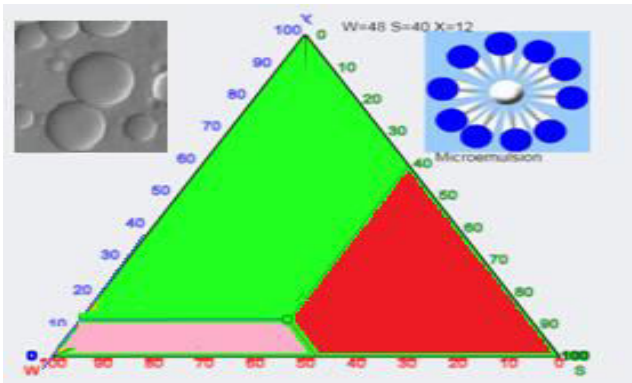


Fig. 1: F1 Pseudoternary phase diagram

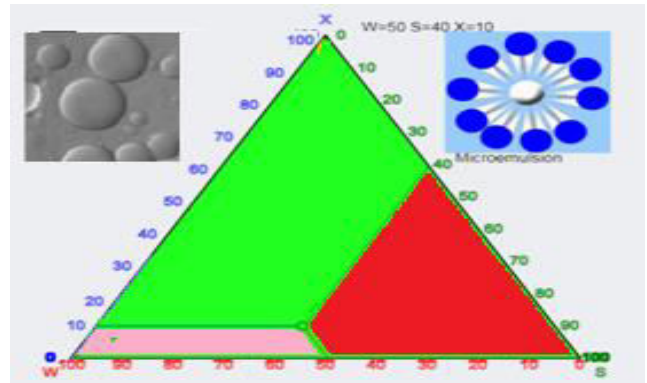


Fig. 2: F2 Pseudoternary phase diagram

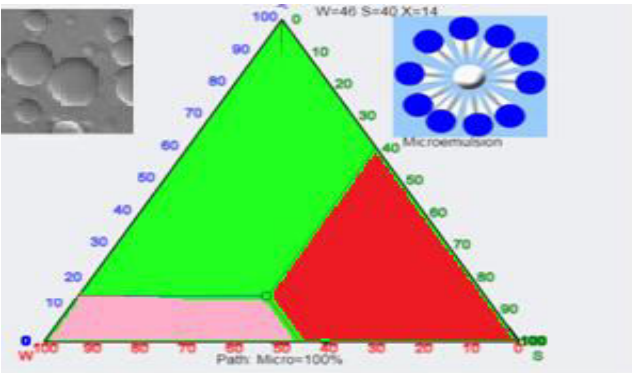


Fig. 3: F3 Pseudoternary phase diagram

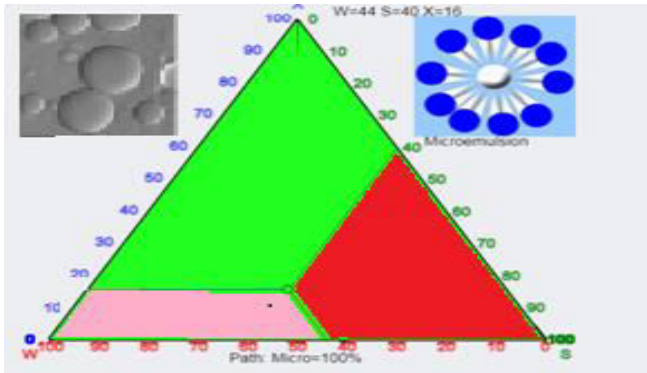


Fig. 4: F4 Pseudoternary phase diagram

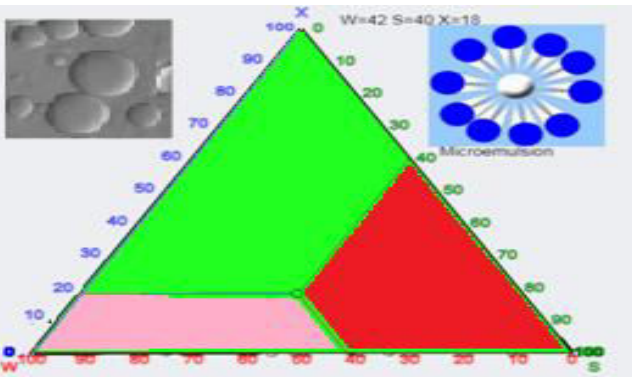


Fig. 5: F5 Pseudoternary phase diagram

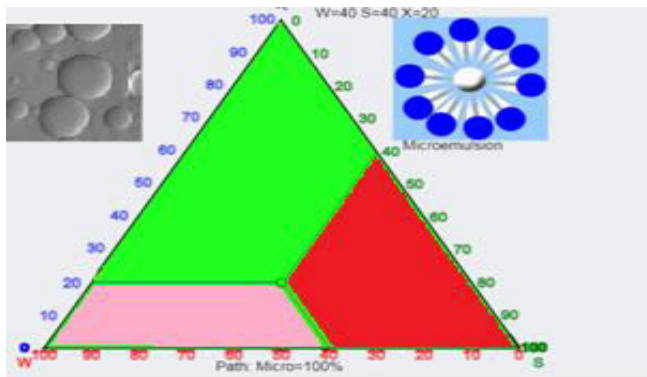


Fig. 6: F6 Pseudoternary phase diagram

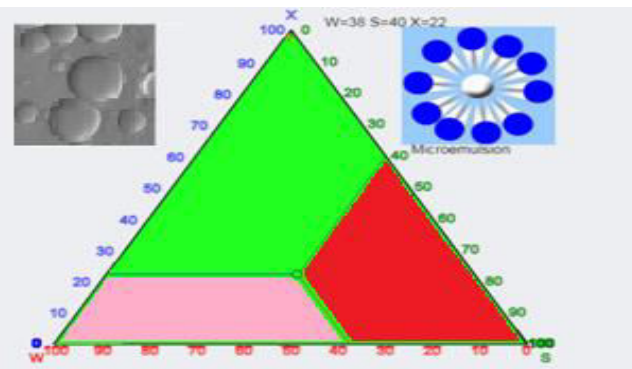


Fig. 7: F7 Pseudoternary phase diagram

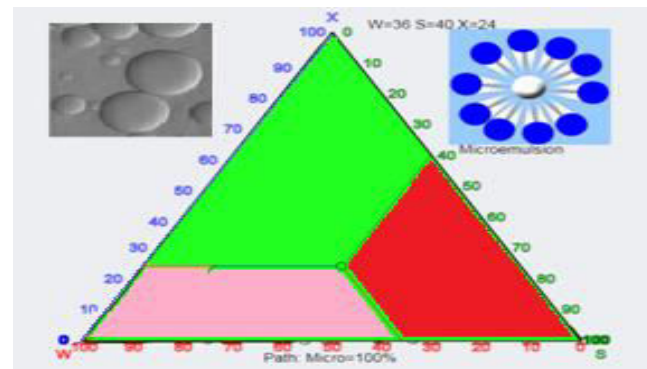
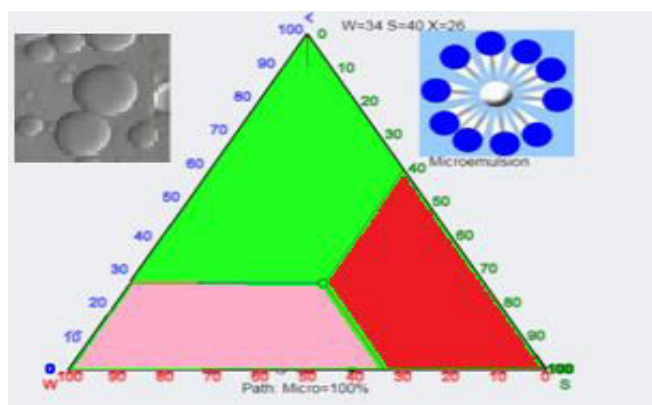


Fig. 8: F8 Pseudoternary phase diagram



**Fig. 9: F9 Pseudoternary phase diagram**

## 2.4. Characterization study of microemulsion

### 2.4.1. Appearance

The prepared batches of microemulsion were visually observed for clarity or any signs of settling. The appearance of the microemulsion formulations was determined by visual inspection of the formulation under light, alternatively on a white and black background, and the turbidity was checked. The test was performed as described in the United States Pharmacopoeia [13].

### 2.4.2. Centrifugation

To eliminate metastable systems, selected microemulsions containing the drug were centrifuged (Research Centrifuge, R-24, Remi Instruments Limited, Mumbai) at 4000 rpm for 4 hours [14].

### 2.4.3. Stress test

These tests were done to upgrade the best microemulsion plan under outrageous conditions. Stress test was carried out at 4°C and 45°C for 48 hours each for a time of six cycles, trailed by 25°C and 21°C for 48 h for around three cycles. The examples were checked for coalescence, cracking or phase separation [15].

### 2.4.4. Refractive index

The refractive index of the system was measured using a simple Abbe refractometer, placing 1 drop of microemulsion on a glass slide [16].

### 2.4.5. Optical clarity (Percentage transmittance)

Transparency of microemulsion plan and its diluted forms (10 and 100 times with distilled water) was controlled by estimating rate conveyance through ultra-violet spectrophotometer (UV-1601-220x, Shimadzu). Rate conveyance of tests was estimated at 301 nm utilizing filtered water as blank [17].

### 2.4.6. Assay

The accurately measured volume (100µl) of the optimized formulation was diluted with methanol to 100 ml and the absorbance was measured at 301 nm using methanol as a blank. The analysis was carried out in triplicate [18].

### 2.4.7. Dilutability and dye solubility test

Dye solubility test done by Water soluble dye, methylene blue solution of 10µl was added to the microemulsion. If the continuous phase water (oil/water emulsion), the colorant will dissolve evenly throughout the system. If the continuous phase is oil (w/o emulsion), the dye will remain as cluster on the surface of the system [19].

### 2.4.8. Viscosity and Surface tension

The rheological properties of the microemulsion were evaluated by Brookfield viscometer with spindle SC 3 even if the system is water in oil (w/o) or oil in water (o/w). If system has low viscosity then it is o/w type of the system and if a high viscosity then it is w/o type of the system. The surface tension of microemulsion was measured at 25°C with a Torsion balance [20].

### 2.4.9. Conductivity measurement

Conductometer (Equip-Tronics, EQ-664, Mumbai, India) was used for determination of the electrical conductivity of the microemulsion. Conductometer equipped with an inbuilt magnetic stirrer. This was done using a conduction cell (with a cell constant of 1.0) contains two platinum plates separated by a desired distance and having a liquid between the platinum plates acting as a conductor [21].

### 2.4.10. Percentage Drug content estimation

A microemulsion containing 100 mg of glyburide was dissolved in 100 ml of 0.1 N. HCl taken in a volumetric flask. Then the solvent was filtered off, 1 ml was taken into 50 ml of a volumetric solution, diluted to the mark with 0.1 N. HCl and analyzed spectrometrically at 301 nm. The concentration of glyburide in mg/ml was obtained using a standard drug calibration curve. Studies of the drug content were carried out in triplicate for each batch of the drug [22].

### 2.4.11. Droplet size distribution and zeta potential Determination

Droplet size distribution, polydispersity index (PDI) and zeta potential of the microemulsion was determined



by using, Nano Malvern droplet analyzer (UK) and zeta potential analyzer. Poly disperse partials have major hurdles in the drug diffusion they reduce the rate of diffusion of the formulation and also due to poly-dispersibility, large partials having a low laplas pressure undergoes Ostwald ripening and aggregation of the particle take place in the formulation. Wavelength scattering angle  $90^\circ$  at  $25^\circ\text{C}$ , average hydrodynamic diameter of the microemulsion was derived from cumulative analysis by the auto-measure software [22].

#### 2.4.12. pH measurement

The pH values of all the formulations were measured by immersing the electrode directly into the dispersion using a calibrated pH meter (Digital Potentiometer Model EQ-601 Equip-Tronics) [23].

#### 2.4.13. Entrapment efficiency and drug loading

Glyburide loaded microemulsion entrapment efficiency was evaluated by a centrifugation method. For a short time,  $10\ \mu\text{L}$  of  $0.1\ \text{mol/L}$  HCl was added into drug-loaded microemulsion and centrifuged for 10 min at 20,000 rpm. The supernatant was separated and the pellets were washed thrice with distilled water. The free drug concentration was determined by UV-visible spectrum photometric analysis at 301 nm. The entrapment efficiency and drug loading were calculated by formula given below. All the measurements were performed in triplicate [13]

Entrapment efficiency (%) =  $[(W_a - W_s) / W_a] \times 100$

Drug loading (%) =  $[(W_a - W_s) / (W_a - W_s + W_l)] \times 100$

Where  $W_a$  is the amount of drug added to formulation,  $W_s$  is the amount of free drug, and  $W_l$  is the weight of oil phase.

#### 2.4.14. Differential scanning calorimetry measurements (DSC)

DSC measurements were performed with DSC TA Q100 instrument equipped with a refrigerated cooling system. Nitrogen with a flow rate of  $50\ \text{ml/min}$  was used as purge gas. Approximately 4 to 13 mg of sample was weighed precisely into hermetic aluminum pans. An empty hermetically sealed pan was used as a reference. The samples were cooled from  $25^\circ\text{C}$  to  $-50^\circ\text{C}$  at a cooling rate of  $5^\circ\text{C} / \text{min}$ , held for 3 min at  $-50^\circ\text{C}$ , and then heated to  $25^\circ\text{C}$  at a heating rate of  $10^\circ\text{C} / \text{min}$ . All the measurements were performed in triplicate [13].

#### 2.4.15. Morphological analysis of Microemulsion by SEM

The outer morphological structure of the microemul-

sion was researched by Scanning Electron Microscopy with a S4800 Type II examining electron microscope (Hitachi high innovations, Japan), working at 15kV. Sample was fixed on a SEM stub utilizing twofold sided adhesive tape and afterward covered with a thin layer of gold. The outer morphological structure of the microemulsion as examined by Scanning Electron Microscopy with a scanning electron microscope (FEI, the Netherlands), working at 15kV. The sample was fixed on a SEM stub utilizing twofold sided adhesive tape and afterward covered with a slim layer of gold [24].

#### 2.4.16. FTIR spectroscopy

It was determined by Fourier Transform Infrared Spectro-photometer (FTIR, Simadzu Corporation). The sample was scanned over wavelength region of  $4000$  to  $400\ \text{cm}^{-1}$  at a resolution of  $4\ \text{cm}^{-1}$  by dispersing sample in KBr and compressing into the disc by applying pressure of 5 tons for 5 min in a hydraulic press. The pellet was placed in light path and the spectrum was obtained [25].

#### 2.4.17. Kinetics of Drug Release

*In vitro* dissolution has been recognized as an important element in drug development. To analyze the mechanism for the release and release rate kinetics of the formulated dosage form, the data obtained from conducted studies was fitted into Zero order, First order, Higuchi matrix, Korsmeyer- Peppas and Hixson Crowell model (Table 1). In this by comparing the r-values obtained, the best-fit model was selected [26].

#### 2.4.18. Stability studies of optimized formulation:

Stability studies were completed for advanced detailing for 6 months at  $37 \pm 2^\circ\text{C}$  and  $04 \pm 2^\circ\text{C}$  as per ICH rule in a controlled chamber. The example was investigated inter-mittently for actual appearance, rheological properties, pH, and rate discharge by UV-Visible spectrophotometer at 301 nm.

### 3. RESULTS AND DISCUSSION

#### 3.1. Pre-formulation Studies

Preliminary studies are performed for understanding physical and chemical properties, behavior of the new drug and possible obstacles in choosing a dosage form development. It generates auxiliary data for necessary changes in design, develop and evaluate formulations. To find out the wavelength maximum absorption ( $\lambda_{\text{max}}$ ) of the drug solution of the drug ( $10\ \mu\text{g} / \text{ml}$ ) in ethanol

was scanned with a spectrophotometer within 400-200 nm wavelength range relative to ethanol as a blank. The curve shows the characteristic absorption maxima at  $\lambda_{max}$  301 nm for glyburide. Calibration curve for evaluation of the prepared product in ethanol, as well as in buffer pH 7.4 as the dissolution media at 301 nm.

**3.2. Solubility study of Glyburide (GLY) in Oil, Surfactants and Co- Surfactants**

Among all screened oils, the most remarkable solubilisation limit was displayed by Capmul MCM (37.551 mg/ml) was chosen for additional examination.

From the results of screening studies, it was observed that, Co Surfactant span-20 found to have very good solubilising capacity compared to Propylene Glycol and *n*-butanol. Span-20 selected co-surfactant also shows good emulsification with selected oil and Tween 80.

**Table 2: Data for Calibration curve**

S.No	Concentration (µg/ml)	Absorbance(nm)
1	2	0.110
2	4	0.201
3	6	0.325
4	8	0.416
5	10	0.512

**Table 3: Solubility study of Glyburide (GLY) in Oil, Surfactants and Co- Surfactants**

Phase type	Excipient	Solubility (mg/ml)	Phase type	Excipient	Solubility (mg/ml)	Phase type	Excipient	Solubility (mg/ml)
Oils	Labrafac CC	32.871	Surfactants	Captex-355	8.871	Co-Surfactants	<i>n</i> -butanol	0.331±0.01
	Capmul MCM	37.551		Cremophor EL	9.551		Propylene glycol	0.231±0.01
	cotton seed oil	28.744		Tween-80	14.744		span-20	7.705±0.02
	sunflower oil	27.545		Labrafil	8.305			
	soybean oil	30.11		PEG 400	7.09			

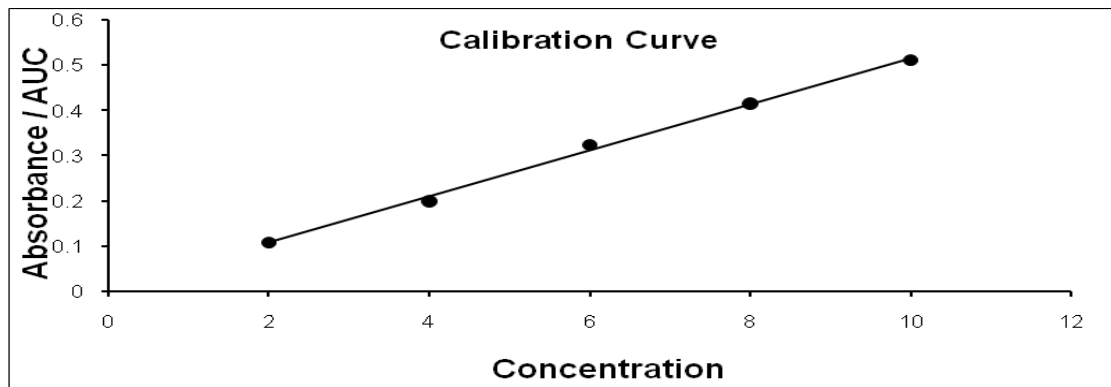


**Fig. 10: Calibration curve**

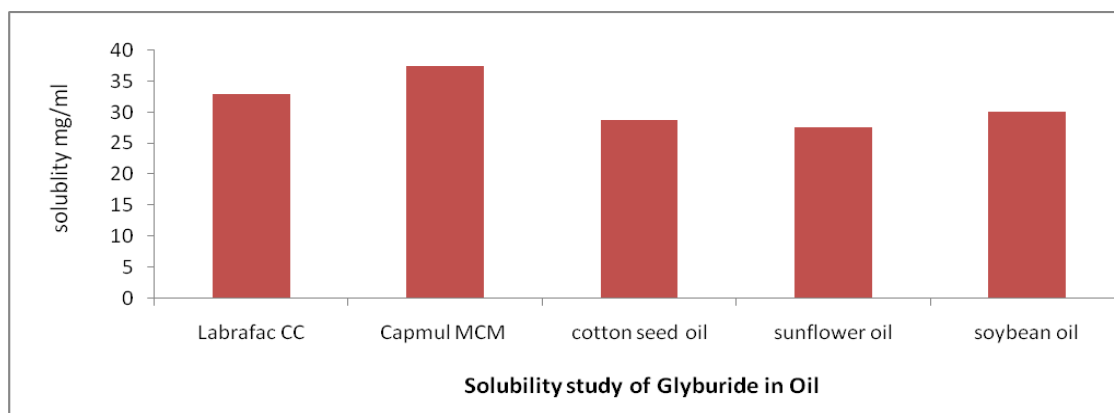


**Fig. 11: Solubility study of Glyburide (GLY) in Oil**

### 3.3. FTIR spectroscopy for Drug-polymer interaction

The spectrum of glyburide showed the following functional groups at their frequencies mentioned. The FT-IR range of the unadulterated medication glyburide was discovered to be like the standard range of glyburide. Further investigation of the similarity of the medication with excipients was explored utilizing FTIR spectroscopy. Pure glyburide shows major peak at IR spectra revealed no considerable change when compared that of glyburide microemulsion formulation proves that there is no drug and excipients interaction. The study of the interaction of excipients with drugs is very important to determine the compatibility of the selected excipients with active drugs. Incompatibility is actually the inactivation of an active drug due to degradation or conversion to a less effective physical or chemical form. When a mixture of two or more active drugs and excipients is mixed together, there is a possibility of interaction in terms of change in appearance, elegance, and, most importantly, the chemical composition of each other. To learn about

chemical changes or interactions, chromatographic, spectroscopic, and thermal analyzes are usually preferred.

### 3.4. Pharmaceutical Evaluation

#### 3.4.1. Physical appearance and Phase separation

The microemulsions were checked for transparency until they were turbid. Microemulsions remained clear when diluted, due to the presence of oils and surfactants microemulsions look transparent/translucent yellow colored solution.

#### 3.4.2. Centrifugation test and stress tests

All formulations detected clearly and there was no sign of precipitation. Centrifugation tests showed that the microemulsion formulations F1, F2, F3, F4, F5, F6 and F7 remained homogeneous without any phase separation. According to the following data, formulations passed through various stress conditions, as shown in table 4. Formulations F1, F2, F3, F4, F5, F6 and F7 passed centrifugation and stress test were stable under all temperature conditions.

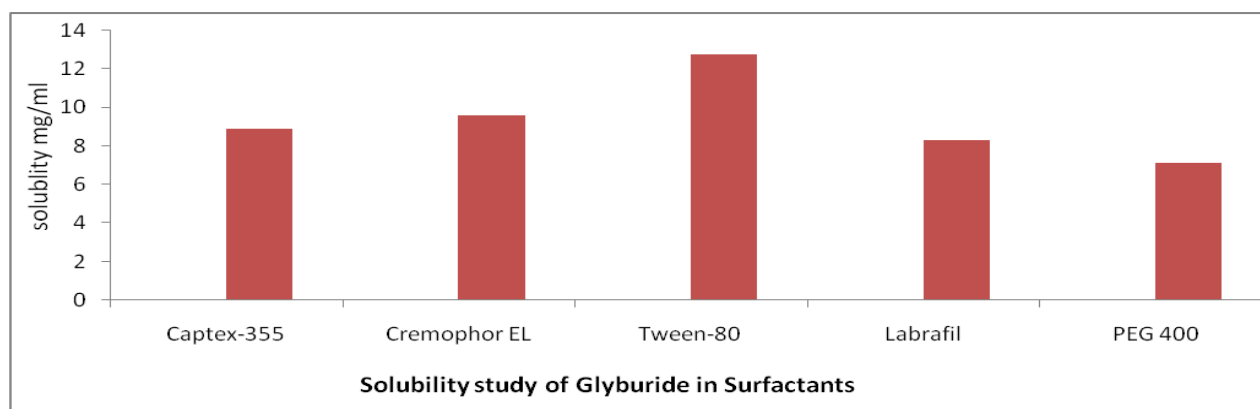


Fig.12: Solubility study of glyburide Surfactants

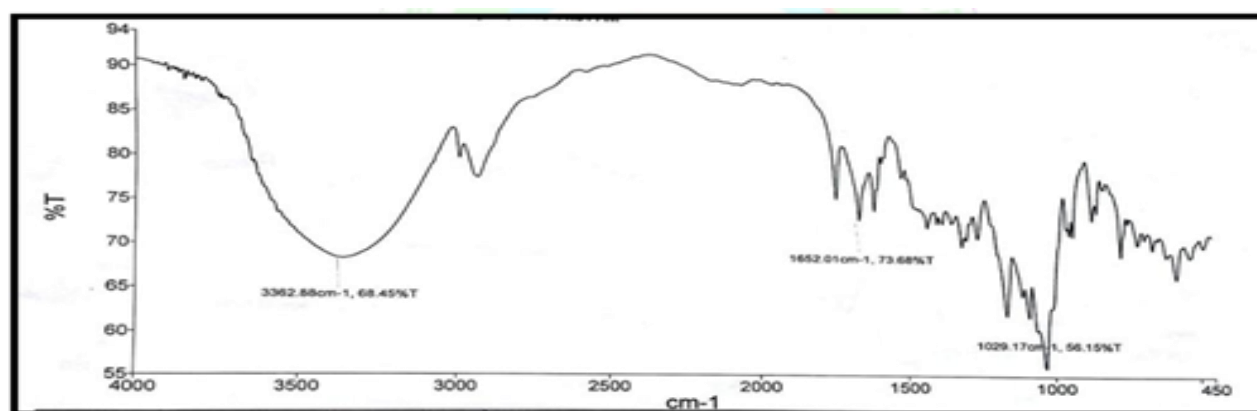


Fig. 13: -FT- IR spectrum of Glyburide

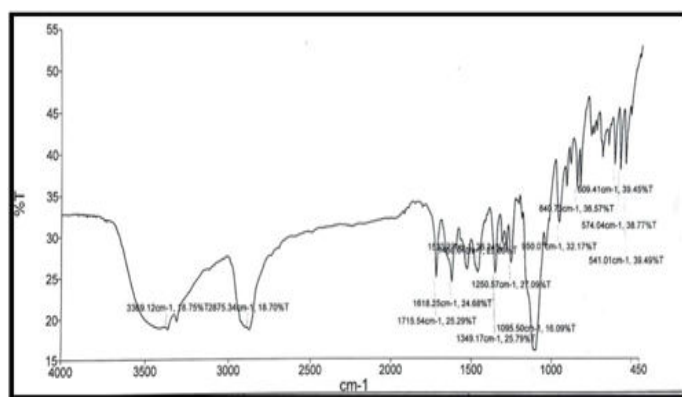


Fig. 14: FTIR spectrum of F3 formulation

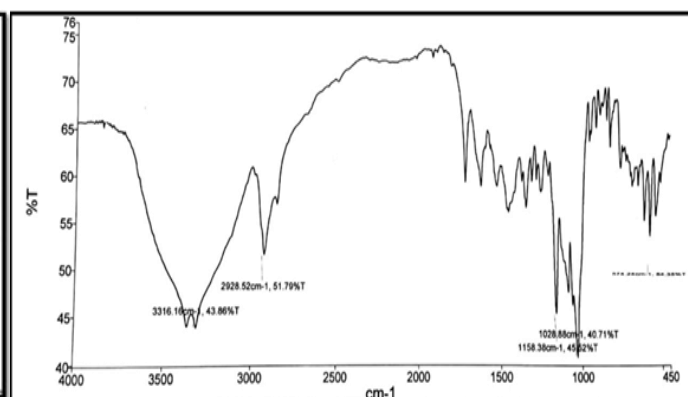


Fig. 15: FTIR spectrum of F5 formulation

Table 4: Results of Physical appearance, Phase separation, Centrifugation test and Observations of stress tests

Formulation code	Physical appearance	Phase separation	Centrifugation test	Observations of stress tests		
				25–30°C	45°C	4°C
F1	Clear Liquid	No	Y	✓	✓	✓
F2	Clear Liquid	No	Y	✓	✓	X
F3	Clear Liquid	No	Y	✓	✓	✓
F4	Clear Liquid	No	Y	✓	✓	✓
F5	Clear Liquid	No	Y	✓	✓	✓
F6	Clear Liquid	No	Y	✓	✓	✓
F7	Clear Liquid	No	Y	✓	✓	✓
F8	Clear Liquid	No	N	✓	X	X
F9	Clear Liquid	No	N	✓	✓	✓

✓ - physically and chemically stable, x- physically and chemically unstable, Y= denote maintenance of homogeneity of prepared microemulsion, N = denote separation of component of microemulsion concentrate

### 3.4.3. Dye-solubility test

Water soluble dye, methylene blue solution was added to optimized microemulsion formulations F1 to F9, the dye will dissolve uniformly throughout the system, so the continuous phase was water. Hence the optimized formulations were found to be o/w type of microemulsion.

### 3.4.4. Viscosity

Microemulsion formulations F1 to F5 shows viscosity value of  $110 \pm 0.51$ cp to  $129 \pm 0.72$ cp Low viscosity of the formulation indicates that formulation is o/w type and having Newtonian flow ensures easy handling and packing.

### 3.4.5. Refractive index

The refractive index of the systems was in the 1.338 to 1.462. It reflects that the microemulsion is almost transparent in the visible spectrum and very little scattering low refractive index.

### 3.4.6. Optical Clarity

The %Transmittance of the systems was found to be in range from 96.2 to 99.2.

### 3.4.7. Surface tension

The surface tension data implies water-in-oil microemulsions because surface tension amounts of microemulsion are nearby to oil phase surface tension.

### 3.4.8. pH

The pH of the composition affects not only the stability of emulsions but also alters the solubility and bioavailability of the drug by emulsion at the point of penetration. The pH of all microemulsion ranged from 5.2 to 6.8 in Table 6 which corresponds to the normal pH range of GIT fluids.

### 3.4.9. Conductivity measurement

The results of measuring electrical conductivity are shown in table 6. Water is a better conductor of



electricity than oil, when the microemulsion contains water in the continuous phase, then the conductivity value is high and it will decrease when the oil is in the continuous phase [27].

#### 3.4.10. Drug Content

Microemulsion equivalent to 10 mg of glyburide was dissolved in an appropriate amount of ethanol (100 ml). The samples were thoroughly mixed to dissolve the drug in ethanol and analyzed using a Shimadzu 1800A UV-Vis spectrophotometer at 301 nm. During the evaluation, the drug content was found to be in the 90.37 to 99.23% range table 6 Optimized lot F3 showed 99.23% drug content.

#### 3.4.11. Droplet size distribution and zeta potential

##### Determination:

Measuring particle size distribution and understanding

how it affects products and processes can be critical to the success of manufacturing. It suggested that the zeta potential can serve as a partial indicator of the physical stability of the resulting emulsions. Most prepared microemulsions should preferably achieve high absolute values of the zeta potential ( $\pm 30$  mV) to ensure the creation of a high energy barrier against coalescence of dispersed droplets. Microemulsion usually has a small particle size ( $< 200$  nm) compared to emulsions [20, 27].

#### 3.4.12. Dissolution study of different batches

The results of *in vitro* dissolution profiles of various glyburide microemulsion formulations are shown in Table. It is evident from the table that glyburide microemulsion showed more than 90% GLY released. The USP recommends pH 7.4 buffers as a dissolution medium for glyburide.

**Table 5: Results of physical evaluation**

Formulation code	Refractive index (RI)	Optical Clarity (% Transmittance)	Assay $\pm$ S.D* (%)	Dye solubility	Viscosity (cp)	Surface tension (dynes/cm)	pH of Formulation
F1	1.426	96.2	96.30 $\pm$ 0.37	✓	116 $\pm$ .12	41.23 $\pm$ 0.61	5.2
F2	1.462	98.2	95.81 $\pm$ 0.26	✓	110 $\pm$ .51	43.53 $\pm$ 1.04	5.5
F3	1.426	97.6	97.04 $\pm$ 0.14	✓	115 $\pm$ .23	41.62 $\pm$ 0.87	6.5
F4	1.438	96.8	91.30 $\pm$ 0.32	✓	122 $\pm$ .13	44.09 $\pm$ 1.53	7.3
F5	1.396	97.2	97.67 $\pm$ 0.02	✓	117 $\pm$ .19	43.61 $\pm$ 1.10	6.2
F6	1.418	99.2	92.21 $\pm$ 0.19	✓	129 $\pm$ .72	42.80 $\pm$ 1.44	5.9
F7	1.462	96.6	88.22 $\pm$ 0.12	✓	119 $\pm$ .17	41.68 $\pm$ 1.22	6.1
F8	1.338	98.4	88.34 $\pm$ 0.45	✓	118 $\pm$ .23	40.78 $\pm$ 1.04	6.3
F9	1.398	96.7	89.91 $\pm$ 0.12	✓	113 $\pm$ .01	38.67 $\pm$ 1.14	6.8

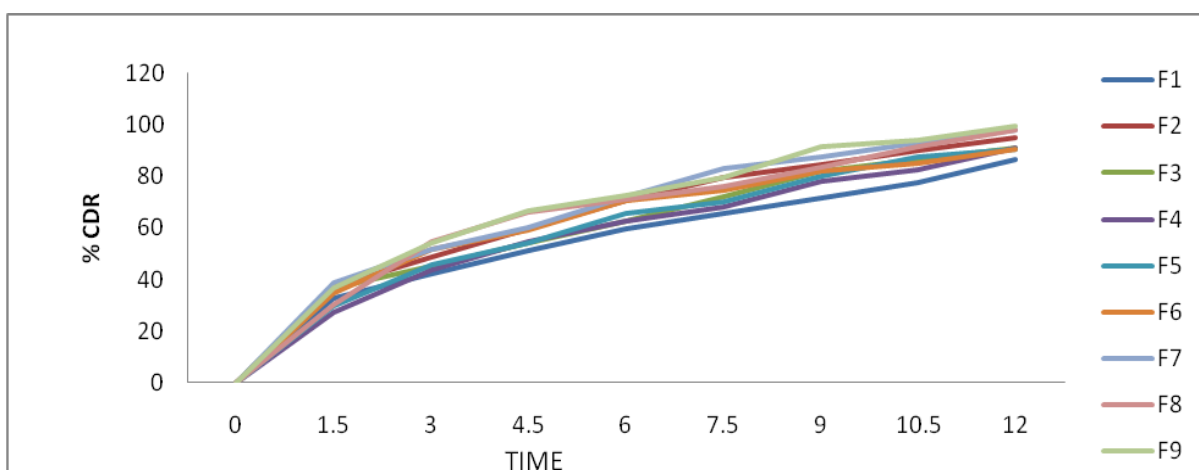
✓ - o/w type of microemulsion

**Table 6: Results of Conductivity, (%) Drug Content, Polydispersity index (PDI), %Drug loading, Entrapment efficiency, (%) Particle size (nm) and Zeta Potential (mv)**

Formulation code	Conductivity	(%)Drug Content	Polydispersity index (PDI)	%Drug loading	Entrapment efficiency (%)	Particle size (nm)	Zeta Potential (mv)
F1	0.183	91.06	0.447	71.12 $\pm$ 0.05	55.5 $\pm$ 2.4	480 $\pm$ 78	26.20 $\pm$ 0.2
F2	0.192	90.56	<b>0.279</b>	73.70 $\pm$ 0.15	73.6 $\pm$ 0.8	625 $\pm$ 55	27.80 $\pm$ 0.4
F3	0.189	99.23	0.368	74.10 $\pm$ 0.71	85.3 $\pm$ 0.8	460 $\pm$ 42	27.90 $\pm$ 0.6
F4	0.199	98.11	0.478	80.23 $\pm$ 0.08	84.3 $\pm$ 3.6	520 $\pm$ 76	28.12 $\pm$ 0.3
F5	0.201	96.10	0.839	77.54 $\pm$ 0.34	85.3 $\pm$ 2.9	360 $\pm$ 12	28.30 $\pm$ 0.1
F6	0.176	95.97	0.575	69.64 $\pm$ 0.34	85.6 $\pm$ 1.2	710 $\pm$ 82	29.40 $\pm$ 0.7
F7	0.180	93.38	0.478	76.30 $\pm$ 0.21	84.9 $\pm$ 1.4	814 $\pm$ 62	31.30 $\pm$ 0.4
F8	0.179	93.71	0.612	70.44 $\pm$ 0.61	84.7 $\pm$ 3.9	650 $\pm$ 59	28.40 $\pm$ 0.3
F9	0.191	90.37	0.536	75.51 $\pm$ 0.92	83.3 $\pm$ 4.5	580 $\pm$ 71	27.23 $\pm$ 0.6

**Table 9: Results of % Drug release of F1 to F9 microemulsion batches**

Time in hours	% Drug release of F1	% Drug release of F2	% Drug release of F3	% Drug release of F4	% Drug release of F5	% Drug release of F6	% Drug release of F7	% Drug release of F8	% Drug release of F9
0	0	0	0	0	0	0	0	0	0
1.5	32.871	37.551	36.744	27.545	29.804	34.640	38.842	30.346	36.762
3	42.555	48.709	45.395	43.501	45.868	51.390	51.540	54.735	54.550
4.5	51.303	59.746	54.541	54.695	54.387	59.010	60.093	65.858	66.856
6	59.599	70.896	62.762	62.762	66.071	70.444	72.101	70.939	72.822
7.5	66.033	79.428	72.284	67.819	70.498	74.517	83.149	76.070	80.013
9	71.854	84.794	82.441	78.030	80.236	82.00	87.440	83.290	91.942
10.5	77.950	90.005	86.665	82.307	87.826	84.922	93.055	91.165	94.069
12	86.742	95.062	91.189	90.902	90.759	90.328	97.931	97.767	96.708

**Fig. 16: Dissolution study of F1 to F9 microemulsion batches**

### 3.4.13. Kinetic of Drug release

To study the release kinetics, data from *in vitro* drug release studies F3 and F5 series glyburide microemulsion formulations showed Higuchi's model as the most suitable. Using the Korsmeyer and Peppas equations, the *n* values were 0.551 and 0.543, respectively table 10. This value is a characteristic of abnormal kinetics (non-Fick transfer) [28-30].

### 3.4.14. Morphological analysis of Microemulsion by SEM

The surface morphology of the glyburide microemulsion was studied using SEM [21]. The images of F3 and F5 shown in fig. 13 and fig.14 shows well-separated particles without agglomeration compared to other batches. Besides particle size, particle shape can also have a significant impact on the performance and handling of many solid particles. Spherical shape particle, without tailing indicates the uniformity of the particle size. In addition, SEM images revealed the

absence of crystalline structure of glyburide in microemulsion formulation [20, 27].

### 3.4.15. Differential scanning calorimetric study (DSC)

Formulation F5 showed endotherms at 123.5°C and 257°C. Placebo composition F5 showed endotherms at 128.6°C and 254.2°C. Tween 80 showed an endothermic effect at 212°C. F3 endotherm at 247°C and placebo endotherm at 254.2°C was associated with the presence of Tween80 in the formulations. No drug peak was observed in F3 and F5 indicating that the drug was completely dissolved in the formulation.

### 3.4.16. Stability studies

Stability studies were completed for advanced detailing for 6 months at 37±2°C and 04±2°C as per ICH rule in a controlled chamber. The example was investigated intermittently for actual appearance, rheological properties, pH, and rate discharge by UV-Visible

spectro-photometer at 301 nm. The physical appearance of the preparation was good without any phase separation or turbidity. The average pH of 5.6, viscosity

of  $122 \pm 0.13$  cps and no considerable change in the percentage release, i.e., 95% was observed for 6 months.

**Table 10: Results of Kinetic of Drug release**

S.No.	R <sup>2</sup> Value					n Value
	Zero order	First order	Higuchi model	Hixson crowell cube root model	Korsmeyer peppas model	
F1	0.993	0.973	0.978	0.989	0.983	0.740
F2	0.980	0.947	0.967	0.975	0.959	0.587
F3	0.927	0.978	0.980	0.976	0.983	0.551
F4	0.959	0.984	0.989	0.979	0.990	0.560
F5	0.922	0.993	0.986	0.993	0.987	0.543
F6	0.886	0.981	0.941	0.930	0.957	0.458
F7	0.982	0.965	0.979	0.980	0.982	0.646
F8	0.875	0.980	0.953	0.933	0.977	0.476
F9	0.903	0.970	0.940	0.910	0.989	0.485

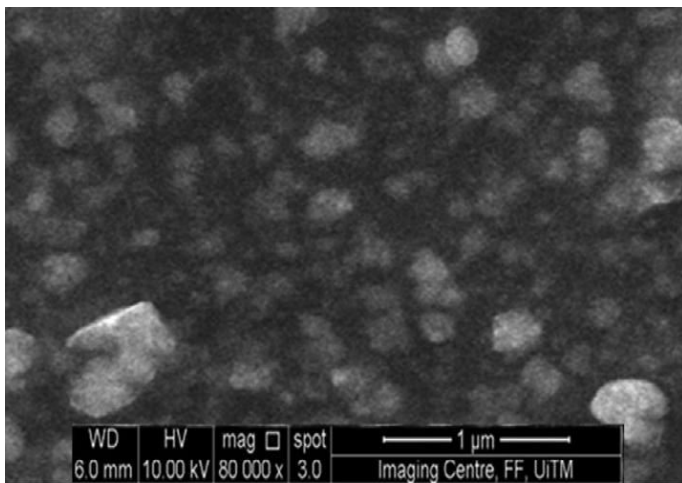


**Fig. 17: Scanning Electron Microscope of F3**

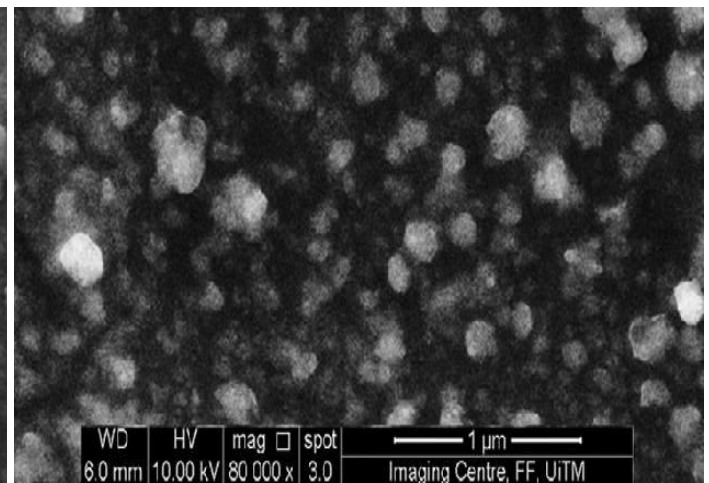


**Fig. 18: Scanning Electron Microscope of F5**

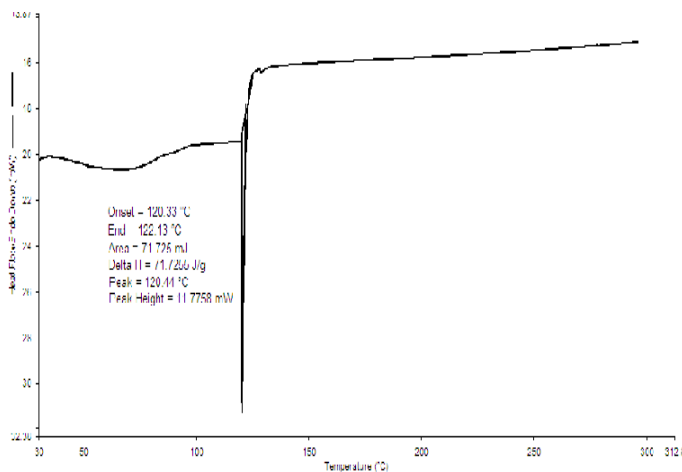


**Fig. 19: DSC of F3**

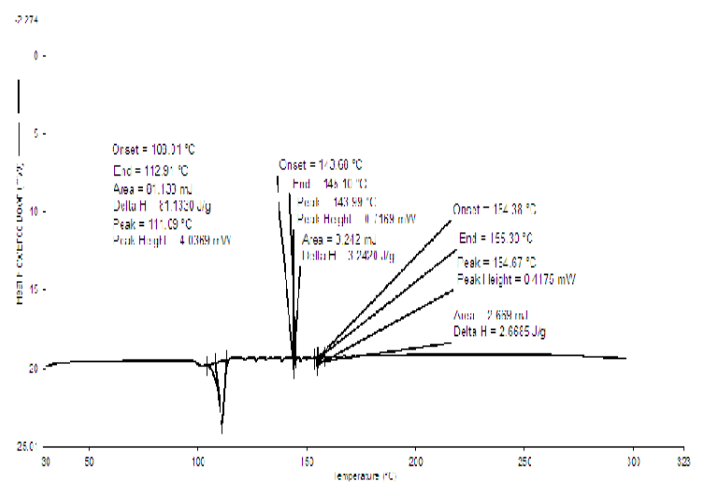


**Fig. 20: DSC of F5**

#### 4. CONCLUSION

Mixing different concentrations of oils significantly increases the solubilizing capacity for poorly water-soluble drug glyburide. This interesting observation was explained by the hypothesis of non-ideal mixing of oils and their penetration into the surfactant layers. The phase diagrams suggest that the composition for administration can be formulated as an oil / surfactant mixture and water-in-oil microemulsions. Nine formulations were prepared which should help improve the bioavailability of poorly soluble drugs. Formulations F3 and F5 containing Capmul MCM, tween 80, Span20 and distilled water selected as best formulation which is a transparent and low viscosity system, with a particle size  $360 \pm 12$ . There is no sign of drug and polymer interaction studied by FTIR. Conductivity studies have revealed structural changes from w/o to o/w through the bicontinuous phase. For the selected compositions, centrifugation test, Stress test, Dye solubility, refractive index, pH, particle size, viscosity, % transmission, zeta potential were studied. F5 were optimized DSC stability studies showed that the formulation was stable. The stability studies confirmed that the optimized microemulsion was stable for six months. Thus, despite of effectiveness of microemulsion based delivery system for improvement of solubility and bioavailability of glyburide, benefits to the risk ratio of the developed formulation via clinical investigation will only decide its suitability in the actual clinical practice. To find out the pharmacokinetic and pharmacodynamic parameters of the optimized drug, additional in vivo testing is required.

#### 5. REFERENCES

1. Groop L, Wahlin-Boll E, Totterman KJ, Melander A, et al. *Eur J Clin Pharmacol.*, 1985; **28**:697-704.
2. Wei H, Lobenberg RL. *Eur J Pharm Sci* 2006; **19**:45-62.
3. Chalk JB, Patterson M, Smith MT, Eadie MJ. *Eur J Clin Pharmacol* 1986; **31**:177-182.
4. Yogeshwar G, Bachhav, Vandana, Patravale, *American Association of Pharmaceutical Scientists*, 2009; **10(2)**:0200-0482
5. Itoh K, Tozuka Y, Oguchi T, Yamamoto K. *Int J Pharm.* 2002; **238**:153-160.
6. Shah NH, Carvajal MT, Patel CI, Infeld MH, Malick AW. *Int J Pharm.* 1994; **106**:15-23.
7. García-Celma MJ, Azemar N, Pes MA, Solans C. *Int J Pharm.* 1994; **105**:77-81.
8. Thevenin MA, Grossiord JL, Poelman MC. *Int J Pharm.* 1996; **137**:177-186.
9. Corsawant CV, Thoren P, Engstrom S. *J Pharm Sci.* 1998; **87**:200-208.
10. Li L, Nandi I, Kim KH. *Int J Pharm.* 2002; **237**:77-85.
11. Patel V, Kukadiya H, Mashru R, Surti N, et al. *Iranian Journal of Pharmaceutical Research.*, 2010; **9(4)**:327-334.
12. Wilson V, Lou X, Osterling DJ, Stolarik DF, et al. *J. Contr. Release.*, 2018; **292**:172-182.
13. Podlogar F, Gasperlin M, Tomsic M, Jamnik A, et al. *Int J Pharm.*, 2004; **276(1-2)**:115-128.
14. Lavanya N, Aparna C, Umamahesh B. *Int J Pharm Pharm Sci.*, **8(8)**:171-176
15. Yadav V, Jadhav P, Kanase K, Bodhe A, Dombe S. *Int J App Pharm.*, 2018; **10(5)**:138-146.
16. Karamustafa F, Celebi N. *Journal of Microencapsulation*, 2008; **25(5)**:315-323.
17. Shailendra Singh Solanki et al. *International Scholarly Research Network, ISRN Pharmaceutics.*, 2012 : Article ID 108164
18. Pavithra DC, Sivasubramaniam L. *Indian J Pharm Sci.*, 2006; **68**:375-376.
19. Divya A, Ch Praveen Kumar, K Gnanaprakash, M Gobinath. *Int J Pharm Rev Res.*, 2014; **4**:1-5.
20. Alany RG, Tucker IG, Davies NM, Rades T. *Drug Dev Ind Pharm.*, 2001; **27(1)**:31-38.
21. Eskandar Moghimipour, Anayatollah Salimi, Soroosh Eftekhari. *Adv Pharm Bull.*, 2013; **3(1)**:63-71.
22. Kale, Deore. *Journal of Young Pharmacists*, 2016; **8(4)**.
23. Ghosh PK, Murthy RS. *Curr Drug Deliv.*, 2006; **3**:167-180.
24. Hintzen F, Perera G, Hauptstein S, Müller C, et al. *Int J Pharm.*, 2014; **10-472(1-2)**:20-26.
25. Henri LR, John LC, David LC, James HW. *J Soc Cosmet Chem.*, 1988; **39**:201-209.
26. Shah BM, Misra M, Shishoo CJ, Padh H. *Drug Deliv.*, 2015; **22(7)**:918-930.
27. Zhu Y, Zhang J, Zheng Q, Wang M, Deng W, Li Q et al. *J Sci Food Agric.*, 2015; **95(13)**:2678-2685.
28. Tandel H, Raval K, Nayani A, Upadhyay M. *J Pharm Bio allied Sci.*, 2012; **4 (Suppl 1)**:S114-S115.
29. Hosny KM, Hassan AH. *Int J Pharm.*, 2014; **475(1-2)**:191-197.
30. Shah BM, Misra M, Shishoo CJ, Padh H. *Drug Deliv.*, 2015; **22(7)**:918-930.